Science of the Total Environment 810 (2022) 152183

Contents lists available at ScienceDirect

Science of the Total Environment

journal homepage: www.elsevier.com/locate/scitotenv

Source tracking of dissolved organic nitrogen at the molecular level during storm events in an agricultural watershed

Most Shirina Begum [a], Mi-Hee Lee [a], Tae Jun Park [a], Seung Yoon Lee [b], Kyung-Hoon Shin [c], Hyun-Sang Shin [d], Meilian Chen [e], Jin Hur [a,*]

[a] Department of Environment and Energy, Sejong University, Seoul 05006, South Korea
[b] K-water Institute, 200 Sintanjin-Ro, Daedeok-Gu, Daejeon 34350, South Korea
[c] Department of Marine Sciences and Convergent Technology, Hanyang University ERICA Campus, Ansan 15588, South Korea
[d] Department of Environmental Energy Engineering, Seoul National University of Science & Technology, Seoul 01811, South Korea
[e] Environmental Program, Guangdong Technion-Israel Institute of Technology, Shantou 515063, China

HIGHLIGHTS

- DOC and DON export increased in rivers in agricultural landscapes during storm events.
- DOM source tracking with optical properties was combined with molecular composition.
- Bayesian mixing approach revealed significant leaching from manure DOM.
- N-containing formulas, polyphenols, and condensed aromatics surged at peak flow.
- >60% unique formulas in the peak flow originating from manure and affected field soil.

GRAPHICAL ABSTRACT

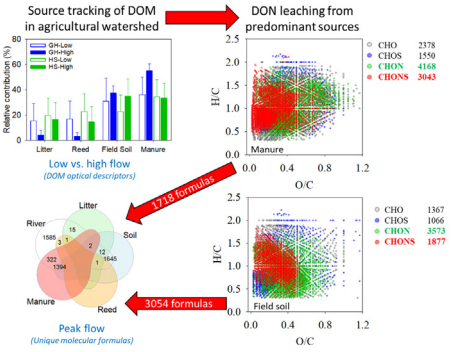

ARTICLE INFO

Article history:
Received 5 October 2021
Received in revised form 29 November 2021
Accepted 30 November 2021
Available online 9 December 2021

Editor: Shuzhen Zhang

Keywords:
Agricultural watershed
Dissolved organic nitrogen
Fluorescence spectroscopy
Bayesian mixing model
FT-ICR-MS

ABSTRACT

Accelerated export of nitrogen-containing dissolved organic matter (DOM) or dissolved organic nitrogen (DON) to streams and rivers from agricultural watersheds has been reported worldwide. However, few studies have examined the dynamics of DOM molecular composition with the attention paid to the relative contributions of DON from various sources altered with flow conditions. In this study, end-member mixing analysis (EMMA) was conducted with the optical properties of DOM to quantify the relative contributions of several major organic matter sources (litter, reed, field soil, and manure) in two rivers of a small agricultural watershed. DOC and DON concentration increased during the storm events with an input of allochthonous DOM as indicated by an increase in specific ultraviolet absorbance at 254 nm ($SUVA_{254}$) and a decrease in biological index (BIX), fluorescence index (FI), and protein-like component (% C3) at high discharge. EMMA results based on a Bayesian mixing model using stable isotope analysis in R (SIAR) were more accurate in source tracking than those using the traditional IsoSource program. Manure (>30%) and field soil (also termed as "manure-impacted field soil") (>23%) end-members revealed their predominant contributions to the riverine DOM in SIAR model, which was enhanced during the storm event (up to 56% and 38%, respectively). The molecular composition of the riverine DOM exhibited a distinct footprint from the manure and manure-

Abbreviations: AImod, Modified aromatic index; BIX, Biological index; CAS, Condensed aromatic structures; DBE, Double bond equivalent; DIN, Dissolved inorganic nitrogen; DOC, Dissolved organic carbon; DOM, Dissolved organic matter; DON, Dissolved organic nitrogen; EEM, Excitation emission matrix; EMMA, End-member mixing analysis; FI, Fluorescence index; FT-ICR-MS, Fourier transform ion cyclotron resonance mass spectrometry; GH, Go-Hyeon River; HIX, Humification index; HS, Ha-Song River; OM, Organic matter; PARAFAC, Parallel factor analysis; SIAR, Stable isotope analysis in R; SRFA, Suwannee River Fulvic Acid; SUVA, Specific ultraviolet absorbance; TDN, Total dissolved nitrogen; TEF, Trophic enrichment factor; WEOM, Water-extractable organic matter.

* Corresponding author.
E-mail address: jinhur@sejong.ac.kr (J. Hur).

http://dx.doi.org/10.1016/j.scitotenv.2021.152183

impacted field soil, with a larger number of CHON formulas and abundant polyphenols and condensed aromatics in peak flow samples in the studied rivers. The riverine DOM during peak flow contained many unique molecular formulas in both rivers (4980 and 2082) of which >60% originated from manure and manure-impacted field soil. Combining the EMMA with DOM molecular composition clearly demonstrated the effect of manure fertilizer on the riverine DOM of the watershed with intensive agriculture. This study provides insights into the source tracking and regulation of DON leaching from anthropogenically altered river systems worldwide.

1. Introduction

Dissolved organic matter (DOM) plays a vital role in the global carbon (C) and other biogeochemical cycles because of its active transformation and exchange across the major Earth systems, namely, the lithosphere, hydrosphere, biosphere, and atmosphere (Aufdenkampe et al., 2011; Bauer and Bianchi, 2011; Cole et al., 2007; Wehrli, 2013). Stream DOM is a complex mixture of autochthonous (algal), allochthonous (plant and soil), and anthropogenic (wastewater and agricultural runoff) organic matter (OM). Thus, the composition and concentration of DOM undergo drastic changes with hydrological, climatic, and anthropogenic disturbances in the watershed (Begum et al., 2019; Knapik et al., 2015; Park et al., 2018). Tracking the sources of OM during storm events has been reported for natural (Jung et al., 2014; Yang et al., 2015b), urban (Lee et al., 2019), and agricultural watersheds (Derrien et al., 2018; Lee et al., 2020; Lee et al., 2019) by using isotopic, spectroscopic, and chromatographic tools (Derrien et al., 2019), in which dissolved organic carbon (DOC) receives most of the attention because of its high abundance.

Notably, studies have highlighted the importance of dissolved organic nitrogen (DON) in aquatic biogeochemical cycles (Li et al., 2018; Osburn et al., 2016; Pisani et al., 2017; Sipler and Bronk, 2015). Particularly, anthropogenic inputs of nitrogen (N) in agricultural watersheds worldwide may lead to significant alterations in the concentration and composition of DOM in streams and pertinent biogeochemical processes (Graeber et al., 2015; Harrison et al., 2005; Hounshell et al., 2017; Pagano et al., 2014; Pellerin et al., 2006). Excessive leaching of N from agricultural watersheds can cause intense eutrophication (Graeber et al., 2015; Smith et al., 1999). Dissolved inorganic N (DIN) is often the main target in watershed management, but DON fractions are also involved in critical environmental problems such as eutrophication, hypoxia, DOM bioavailability, and greenhouse gas (i.e., N_2O) emissions (Chun et al., 2020; Li et al., 2018; Osburn et al., 2016). Organic N accounts for 12–94% of the riverine dissolved N pools (Li et al., 2016; Pisani et al., 2017; Sipler and Bronk, 2015). Studies have reported the export of DON from DIN transformation by plants and microbes, reemphasizing the importance of incorporating DON in N biogeochemistry research (Lewis et al., 2011; Li et al., 2018). The intrinsic properties of OM control the stability of DOM in inland waters, whereas a significant fraction of DON, namely, amino acids, urea, and amino sugars, are considered bioavailable to the in situ microbial community (Bronk et al., 2007; See et al., 2006; Seitzinger et al., 2002).

Advanced techniques such as Fourier transform ion cyclotron resonance mass spectrometry (FT-ICR-MS) analysis have been applied to characterize the molecular composition of DOM in urbanized (Begum et al., 2019; Lusk and Toor, 2016; Ye et al., 2019; Zhang et al., 2021) and agricultural rivers (Li et al., 2018; Luek et al., 2020; Spencer et al., 2019). The high-resolution molecular composition showed an abundance of N- and S-containing formulas in anthropogenically modified rivers and streams, including urban and agricultural watersheds (Li et al., 2018; Lusk and Toor, 2016; Zhang et al., 2021). Spectroscopic analysis has shown that agricultural streams contain abundant protein-like DOM and are highly biodegradable compared with undisturbed waters (Begum et al., 2019; Bida et al., 2015; Chen et al., 2020; Graeber et al., 2015; Li et al., 2018; Wilson and Xenopoulos, 2009). Spectrometric methods are more feasible for routine DOM monitoring but lacks molecular specificity; therefore, ultrahigh resolution FT-ICR-MS analysis has become popular for its high molecular specificity (McCallister et al., 2018). However, FT-ICR-MS analysis, which provides DON molecular composition at an ultrahigh-resolution, has rarely been used to study the agricultural export of DON (Li et al., 2018). Li et al. (2018) reported the spatial variability and transformation of DON molecular composition in agricultural drainage channels. However, this source tracking of DON by linking molecular formulas between river water and upstream end-members is scarce in agricultural watersheds.

To identify the predominant sources of riverine DOM during storm events, many studies have relied on a qualitative analysis based on a comparison of the optical, molecular, and isotopic descriptors of DOM between river samples and various end-members in the watershed (Inamdar et al., 2011; Lee et al., 2016; Yang et al., 2015a). The more recent studies have applied quantitative approaches such as linear mixing models to estimate the relative contributions of potential DOM sources or end-members in the catchment using optical, molecular, and spectroscopic descriptors of DOM (Lee et al., 2020; Lee et al., 2019; Yang et al., 2015a). The traditional linear mixing model approach using the IsoSource program has been frequently used because of its simplicity; however, this model does not account for the potential variability of DOM descriptors in the end-members. Bayesian mixing models have emerged as an effective DOM source tracking method in R, using the "stable isotope analysis in R" (SIAR) package, to overcome the limitation but have been constrained to isotopic descriptors (Menges et al., 2020; Parnell et al., 2010).

In this study, we make a first attempt with end-member mixing analysis (EMMA) using the Bayesian mixing model approach in SIAR using optical descriptors of DOM because this approach is suitable for considering the variability within each end-member. Isotopic descriptors (e.g., ^{13}C, ^{15}N, and ^{18}O) are preferred for higher accuracy in the source tracking of simpler moieties in multiple processes (e.g., nitrate and sulfate sources, plant water uptake, and animal diet) (Tewfik et al., 2016; Wang et al., 2019; Xue et al., 2012; Zhang et al., 2020). However, optical descriptors are simpler and cost-effective for the analysis of complex targets such as DOM using EMMA. Furthermore, SIAR models with isotopic descriptors require trophic enrichment factors (TFEs) or discrimination factors, useful for studying the trophic level or diet of animals but not applicable in source tracking of DOM by optical descriptors (Parnell et al., 2010; Wang et al., 2019). Unlike a limited number of isotopes, many optical descriptors can discriminate well among various DOM sources in different anthropogenically altered watersheds (Derrien et al., 2018; Lee et al., 2020; Lee et al., 2019; Yang et al., 2015a), allowing feasible, accurate source tracking of DOM by a Bayesian mixing model (SIAR). Despite many advantages, EMMA with DOM optical descriptors is not sufficient to explore DON export from agricultural watershed; therefore, DOM molecular composition is necessary for comprehensive understanding of DON.

Continuing our studies on source tracking of DOM and particulate OM in headwater, agricultural, and urban watersheds (Derrien et al., 2018; Derrien et al., 2020; Lee et al., 2020; Lee et al., 2019; Yang et al., 2015a), we aim to provide the first assessment of DON source and composition by combining optical and molecular techniques in an agricultural watershed during monsoon storm events. The main objective of this study was to characterize the molecular composition of DON in runoff water from two rivers flowing through agricultural catchments. Specifically, we tested the hypotheses that (1) the stream DOM receives a large input of DON from the upstream agricultural watershed during storm events and (2) the optical and molecular composition of DOM can provide a holistic view of agricultural alteration in the source and composition of DON. According to our review of the literature, this report is the first on source tracking of DON in runoff water from agricultural drainage channels using EMMA with optical and molecular analyses.

2. Materials and methods

2.1. Study site

The study sites are located at the most downstream reaches of two rivers, the Go-Hyeon River (GH) and the Ha-Song River (HS), which flow into the recently constructed Bohyunsan dam reservoir in South Korea (36°7′33.93″ N, 128°56′56.29″ E) (Fig. S1). The total catchment area of the watershed is 32.61 km^2. The predominant land use of the watershed includes 80% forest and 12% agricultural land (Table S1) (Lee et al., 2020). The typical weather in South Korea is characterized by a summer monsoon from late June to September, followed by a long low-flow period until March. Similar patterns were observed in 2019 at a nearby weather station, accounting for 61% of the annual precipitation (1038 mm) during the monsoon.

2.2. Sample collection

Water samples were collected from the mouths of the GH and the HS before entering the Bohyunsan Reservoir from June 26 to 30, 2019 (Fig. S1). The samples were classified into two categories, "low flow" and "high flow" based on hydrometeorological conditions such as rainfall, discharge, water level, and turbidity (HACH turbidimeter) (Fig. 1). Water levels used to separate the low- and high-flow periods differed for the two rivers because of the different hydrological conditions. For example, the water levels representing a low-flow period were 0.57 m for the GH and 0.22 m for the HS, and the high-flow water levels were 0.73 m and 0.26 m, respectively (Fig. 1).

The preparation process of the DOM source end-member was performed as described by Lee et al. (2020). Based on a preliminary survey of the upper catchments, collection in triplicate was performed for potential organic source materials that might influence the downstream DOM, including fallen deciduous broad leaves (e.g., beech, chestnut tree, oak, royal foxglove tree) in forest, riparian reeds (*Phragmites communis*), field soil, and manure, often used for compost in this watershed area (Fig. S1) (Lee et al., 2020). The organic source materials were oven-dried at 45 °C for three days. The dried plants were cut into pieces of about 1 cm^2 before grinding. The soils were sieved with a 2-mm sieve. The dried manure was finely pounded into a mortar. The water-extractable OM (WEOM) from each organic source material was obtained as the DOM source end-member by mixing the materials with Milli-Q water at a solid-to-solution ratio of 1:10 for the soil and manure samples or 1:20 for the plant samples. Mixing was performed for 24 h at 130 rpm at room temperature (~25 °C). Before filtration, the WEOM was centrifuged at 8000 rpm for 10 min. The supernatants were finally filtered through pre-ashed 0.7-μm GF/F filters (Whatman).

2.3. Analytical methods

2.3.1. Concentrations and optical properties of DOM

The concentrations of DOC and total dissolved nitrogen (TDN) were measured in filtered water samples (pre-ashed GF/F; 0.7 μm) using a total

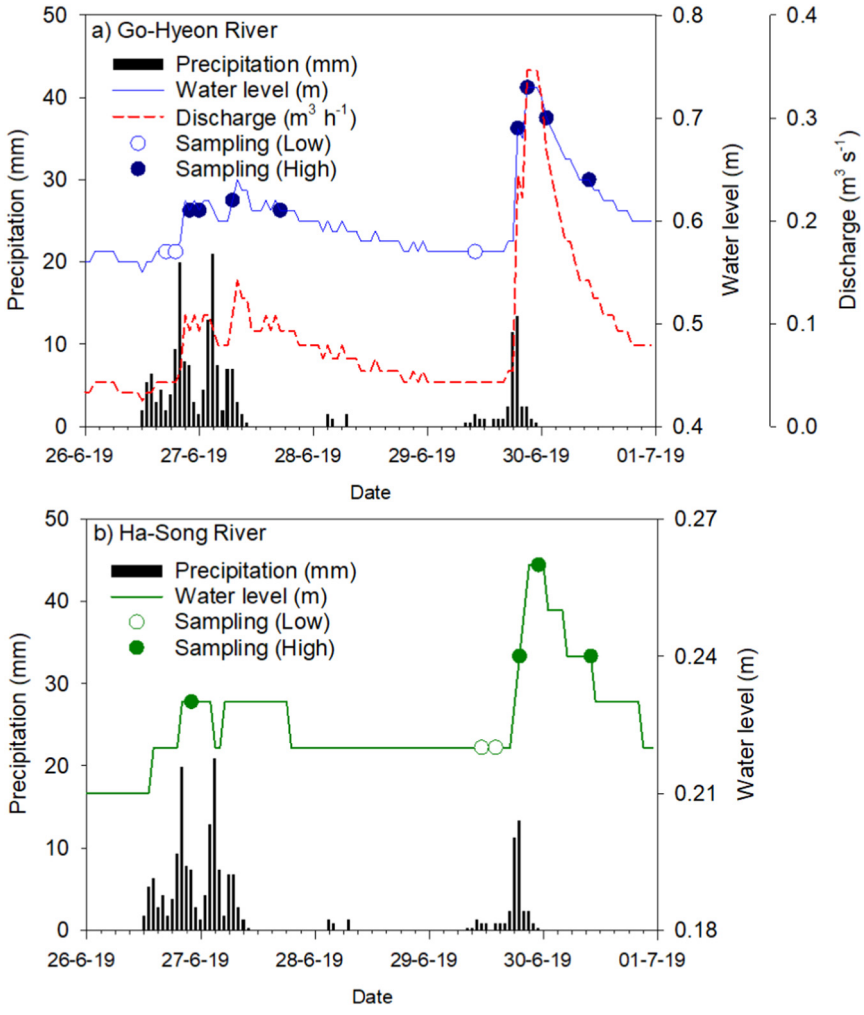

Fig. 1. Hydrograph of storm events including precipitation, water level, and discharge in the Go-Hyeon River (a) and Ha-Song River (b). Samples collected during low and high flow are indicated by void and filled circles, respectively.

organic C and N analyzer (TOC-VCPN, Shimadzu, Japan). Suspended solids (SS) were measured as the difference between the filter weights before and after filtering and drying at 60 °C for 48 h. The concentrations of nitrite-N (NO_2^--N), nitrate-N (NO_3-N), and ammonium-N (NH_4^+-N) were measured using ion-exchange chromatography (790 Personal IC, Metrohm, Switzerland). DON concentration was calculated by subtracting the DIN species (NH_4^+-N, NO_2-N, and NO_3-N) from the TDN (DON = TDN – DIN). Absorption spectra from 200 to 600 nm were scanned at 1 nm intervals by an ultraviolet (UV)–visible spectrophotometer (UV-1800, Shimadzu, Japan). The specific UV absorbance ($SUVA_{254}$) was calculated based on the decadic UV absorption coefficient at 254 nm divided by the DOC concentration (Weishaar et al., 2003).

Fluorescence excitation-emission matrices (EEMs) were recorded using a luminescence spectrometer (F-7000, Hitachi, Japan) at an emission wavelength (Em) of 280–550 nm with 1 nm resolution by stepwise increasing the excitation wavelength (Ex) from 220 nm to 500 nm at 5 nm. The excitation and emission slits were adjusted to 10 nm. The fluorescence response to distilled water were subtracted from the measured spectra to obtain the final EEM data of the DOM samples. Samples for measurements were diluted until the UV absorption coefficient at 254 nm dropped below 0.05 cm^{-1} to minimize the inner-filter effects (Ohno, 2002). The samples were rescaled to account for dilution. Raman units (R.U.) were used to represent fluorescence intensities (Lawaetz and Stedmon, 2009). Common fluorescence descriptors, including the fluorescence index (FI), humification index (HIX), and biological index (BIX) values, were calculated according to the definitions described in the Supplementary Information (Table S2) (Huguet et al., 2009; McKnight et al., 2001; Zsolnay et al., 1999). The major fluorescent DOM (FDOM) components were decomposed from the corrected EEMs by parallel factor analysis (PARAFAC) in MATLAB software (MathWorks, Natick, USA) using the DOMFluor toolbox (Stedmon and Bro, 2008).

2.3.2. FT-ICR-MS analyses

For solid-phase extraction (SPE), river water, and WEOM samples were adjusted to pH 2.0. The sample was discharged through a pre-washed SPE cartridge at a flow rate of 10 mL min^{-1} and then eluted with 6 mL of methanol. The same steps were performed for the blank sample. Eluted samples were stored at −20 °C until the FT-ICR-MS analysis (Chen et al., 2016; He et al., 2016).

Ultrahigh-resolution mass spectrometry measurements were performed by a 15 T FT-ICR-MS interfaced with an Apollo II electrospray ionization source (15T-FT-ICR-MS, Bruker Daltonik, Germany), located at the Korea Basic Science Institute in Ochang, South Korea. A negative ion mode (NanoMate, Advion Biosciences, USA) was used because the DOM is usually negatively charged. The instrument was operated in the broadband mode between 150 and 1200 *m/z*. Samples were injected using a Hamilton syringe at a flow rate of 2 μL min^{-1}. The spray current was set to −3.0 kV, and the drying gas temperature was 180 °C with a 4.0 L min^{-1} flow rate. The skimmer voltage was set to −30 V. One hundred transient scans, collected with a 4 MWord time domain, were co-added to one mass spectrum. External calibration with arginine clusters and internal recalibration with Suwannee River Fulvic Acid (SRFA) as a built-in mixture was adopted to achieve a mass accuracy of <0.050 ppm. Procedural blanks were obtained and subtracted from each corresponding sample. A conservative magnitude threshold was set to an S/N ratio >10 to avoid potential false positives. All ions were singly charged, confirmed by the isotopic spacing pattern (1.00335 Da) of the corresponding $^{12}C_n$ and $^{13}C_{12}C_{n-1}$ mass peaks. Spectra were evaluated in the mass range of 200–800 *m/z*. The mass accuracy threshold was $|\Delta m| \leq 2$ ppm. The nitrogen rule and double bond equivalent (DBE = 1 + 1/2(2C − H + N)) rule (permitting only positive integers) were applied (Koch and Dittmar, 2006). The criteria of elemental ratios were implemented as 2.25 > H/C > 0.3, O/C < 1.2, N/C < 0.5, and S/C < 0.2. Several selected indices, such as the intensity-weighted average (wa) molecular masses, elemental ratios, modified aromatic index (AI_{mod} = (1 + C − 0.5O − S − 0.5(N + H)) / (C − 0.5O − N − S)), and DBE were calculated from the normalized peak intensities (Koch and Dittmar, 2016). Assigned formulas were classified into five compound groups: aliphatics, peptides, highly unsaturated hydrocarbons, polyphenols, and condensed aromatic structures (CAS) (Chen et al., 2021; Spencer et al., 2014). The detailed criteria of the implemented elemental ratios of the five groups are listed in Table S3 (Chen et al., 2021).

2.4. EMMA

Relative contributions of the collected DOM end-members to the river waters were estimated using the SIAR package in R, based on a Bayesian mixing model. SIAR and other Bayesian mixing models have been successfully applied for source partitioning of consumers' food by using C, N, and other stable isotopes (Menges et al., 2020; Parnell et al., 2010). Stable C and N isotopic composition of the end-members are included in the supporting Information (Table S4) from a previous study on the same watershed (Lee et al., 2020). In this study, we attempted a SIAR model with optical properties of DOM instead of stable isotopes and set the trophic enrichment factor (TEF) to zero. Two optimum DOM optical parameters were selected for the analysis by following established criteria in the literature (Derrien et al., 2018; Lee et al., 2019; Yang et al., 2015a; Yu et al., 2019). In brief, DOM optical parameters were excluded if the storm sample exceeded the range of the end-members. Discriminatory analyses, such as *t*-tests, were also conducted between the low- and high-flow river samples. Student's *t*-test was conducted if the data followed a normal distribution (Shapiro–Wilk test), and Mann–Whitney Rank Sum Tests were applied otherwise (SigmaPlot version 14.5). The two best candidates were chosen for the model based on the p values of the *t*-tests. The values of the selected parameters in the riverine DOM (mixture), end-member DOM (sources), and TEF (fractionation corrections) were used as the input parameter. The model fitting via Markov Chain Monte Carlo simulation is known to produce plausible values for end-member contribution to the riverine DOM, and outputs are presented as the average and standard deviations. The model output also includes a posterior distribution representing a true probability density for the selected parameters, which is used to evaluate model performance (Parnell et al., 2010). Because the application of this approach is the first attempt, a more common linear mixing model approach with IsoSource was also conducted. The same set of DOM optical parameters was used in the IsoSource program with a source increment of 3% and a mass balance tolerance of 1‰.

3. Results and discussion

3.1. Water quality during low and high flow

3.1.1. Rainfall and storm events

Two consecutive storm events had a cumulative rainfall of 190 mm. Water levels measured during the sample collection ranged from 0.57 m to 0.73 m and from 0.22 m to 0.26 m in the GH and the HS, respectively (Fig. 1). The short lag time between rainfall and discharge suggests a short water retention time in the small watershed and the dominance of surface runoff. SS and turbidity increased during the storm events (1357 mg L^{-1} and 1569 NTU, respectively) by two orders of magnitude from the base flow (2 mg L^{-1} and 3 NTU) (Table S5).

3.1.2. C and N concentrations

DOC concentrations were highly variable during the storm events with an average of 3.85 mg L^{-1} (2.60–8.11 mg L^{-1}), with higher levels during the high-flow than the low-flow period in the GH and the HS (Fig. 2; Table 1). Similar observations of an increase in DOC were reported in rivers during storm events (Lee et al., 2019) and monsoon seasons (Ittekkot et al., 1985), attributed to the input of allochthonous OM from soil and terrestrial systems (Lee et al., 2019; Raymond et al., 2016). Additionally, TDN and NO_3^- concentrations in the HS were significantly lower ($p < 0.05$) during the high-flow period (3.32 and 2.17 mg L^{-1}, respectively) than the low-flow period (6.41 and 5.38 mg L^{-1}). Although the use of manure fertilizer in agricultural watersheds might lead to increased N concentrations in

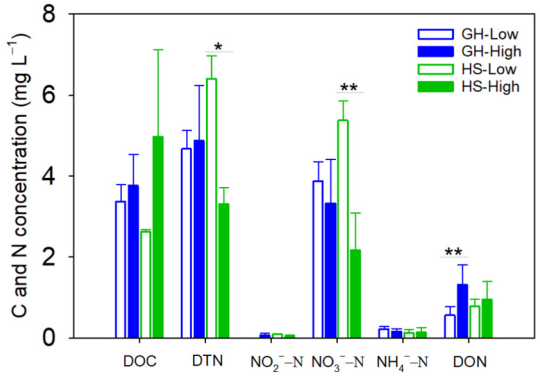

Fig. 2. Mean C and N concentrations during low and high flow in the Go-Hyeon (GH) and Ha-Song (HS) rivers in the agricultural Bohyunsan watershed. Significant differences between the low- and high-flow samples at $p < 0.05$ and $p < 0.01$ are indicated by * and **, respectively.

monsoonal rainfall or winter snowmelt (Jiang et al., 2014; Luek et al., 2020), enhanced microbial activity, shorter water retention time, and plant uptake could lower the TDN and NO_3^--N concentrations during storm events (Jiang et al., 2014). DON concentration was significantly higher ($p < 0.01$) during the high-flow period (1.32 mg L^{-1}) in the GH than in the low-flow period (0.57 mg L^{-1}), whereas the increase in the HS was not statistically significant (Fig. 2; Table 1). Higher DON concentrations were also reported in agricultural runoff with inputs of organic and inorganic fertilizers compared with runoff without fertilizer (Li et al., 2018). The concurrent increase in DOC and DON concentrations suggests that significant amounts of allochthonous DOM may enter rivers with a significant fraction of DON from disturbances in the landscape such as tilling, cropping, and applying fertilizer (Graeber et al., 2015). While DOC and DON export exceeded the dilution effect during storm events in the riverine DOM, relatively smaller amount of inorganic C or N export was probably offset by dilution from rainfall and discharge.

3.2. Dynamics of DOM optical descriptors

3.2.1. Fluorescent DOM components

Three FDOM components (C1, C2, and C3) were identified using PARAFAC modeling. C1, C2, and C3 were assigned to humic-like (C1), terrestrial humic-like (C2), and protein-like (C3) components (Fig. S2) based on similarities with the peaks reported in the literature (Cory et al., 2010; Fellman et al., 2010; Lee et al., 2020). The FDOM components were also matched with the OpenFluor database (Murphy et al., 2014), and 214, 62, and 110 matches were found for the C1, C2, and C3 components, respectively (Table S6). The intensity of the FDOM components, relative to the total fluorescence, termed %C1, %C2, and %C3, is presented in this study as optical descriptors of allochthonous and autochthonous DOM in the rivers and end-members.

3.2.2. Characteristics of end-members

DOC concentrations in the WEOM of the end-members were variable among litter (40.50 mg g^{-1}), reed (41.00 mg g^{-1}), field soil (0.16 mg g^{-1}), and manure (14.50 mg g^{-1}) (Table 1). DON concentrations in the end-members were in the following order: reed (3.48 mg g^{-1}) > manure (1.83 mg g^{-1}) > litter (0.54 mg g^{-1}) > field soil (0.02 mg g^{-1}) (Table 1). $SUVA_{254}$ and HIX were the highest in the field soil (5.38 L mg C^{-1} m^{-1} and 11.89), followed by manure (4.89 L mg C^{-1} m^{-1} and 3.35) (Table 1). The much higher HIX in field soil suggests intense humification of DOM in the soil as opposed to manure, although both end-members have a predominant aromatic fraction, indicated by high $SUVA_{254}$ (Inamdar et al., 2012; Yang et al., 2015a). The lower values of BIX and FI in field soil indicate insufficient presence of biologically produced fresh DOM, whereas the higher values in manure suggest the state of its early composting phase when the manure-derived DOM is exported (Lee et al., 2020). Humification of DOM in field soil was also evident by its higher %C2 (61%) and lower %C1 and %C3 (Fig. S3; Table 1), consistent with studies that reported a predominant contribution from terrestrial DOM in soil leachate (Derrien et al., 2018; Derrien et al., 2020; Lee et al., 2020). By contrast, manure DOM contained higher amounts of humic- (%C1: 42%) and protein-like (%C3: 37%) components and was depleted in terrestrial humic-like DOM (Fig. S3; Table 1). Even though humic-like DOM is usual in soil and terrestrial sources, other sources including manure can also contain a small fraction of humic-like fluorophores (Zhang et al., 2012).

Litter and reed end-members exhibited different DOM compositions from field soil and manure counterparts with very high %C3 and low $SUVA_{254}$, suggesting the presence of labile DOM with only small fractions of humic-like substances and aromatic content (Derrien et al., 2020; Lee et al., 2020). Additionally, the lower HIX in the reed-derived DOM (0.29) than in the litter-based DOM (1.09) suggests that the reed end-member did not undergo humification as much as the litter end-member. The latter showed a lower BIX (0.37) and FI (1.54) than the former, indicating a lack of biological and/or fresh DOM in litter end-members (Table 1). Our findings are in line with studies reporting a relatively higher level of humification in leaf litter and soil DOM, a labile protein-like content in reed DOM, and the dominance of fresh biological products in manure-derived DOM (Derrien et al., 2020; Inamdar et al., 2011; Lee et al., 2020; Lee et al., 2019).

3.2.3. Characteristics of riverine DOM

Optical characteristics of the river water samples showed dynamic changes between the two rivers under different flow conditions. $SUVA_{254}$ increased from low to high flow in the GH (range: 2.68–6.01 L mg C^{-1} m^{-1}) and HS (range: 2.76–5.41 L mg C^{-1} m^{-1}) (Table 1). The concomitant increase in DOC concentration and $SUVA_{254}$ indicates that

Table 1
Dissolved organic carbon (DOC) concentration and optical descriptors of the river samples and four end-members in the Bohyunsan watershed. The section criteria and selected dissolved organic matter (DOM) optical descriptor for the end-member mixing analysis are indicated in bold font at the bottom row.

		DOC [mg g^{-1}]	DON [mg g^{-1}]	$SUVA_{254}$ [m^2 g^{-1}]	HIX	BIX	FI	%C1	%C2	%C3
End-members (n = 3)	Litter	40.50	0.54	2.18	1.09	0.37	1.54	25	14	61
	Reed	41.00	3.48	1.04	0.29	0.67	1.76	14	4	82
	Field soil	0.16	0.02	5.38	11.89	0.44	1.41	27	61	13
	Manure	14.50	1.83	4.89	3.35	0.75	1.93	42	21	37
		[mg L^{-1}]	[mg L^{-1}]							
Go-Hyeon River (n = 11)	Average	3.66	1.11	4.66	5.40	0.81	1.74	55	22	23
	Minimum	2.86	0.38	3.08	4.33	0.73	1.67	50	16	20
	Maximum	4.82	2.00	6.92	6.75	0.89	1.82	64	27	27
Ha-Song River (n = 6)	Average	4.19	0.91	4.21	6.56	0.76	1.70	54	26	20
	Minimum	2.60	0.59	3.18	4.07	0.61	1.59	46	19	13
	Maximum	8.11	1.43	6.23	8.39	0.81	1.79	60	37	28
Validated range				X	O	X	O	X	O	O
t-Test, p-value (low vs high)				0.016	0.165	0.370	0.004	<0.001	0.206	0.011
				Rejected	Rejected	Rejected	**Selected**	Rejected	Rejected	**Selected**

allochthonous DOM rich in aromatic content entered the river from upstream catchments during storm events (Ittekkot et al., 1985; Lee et al., 2019; Yang et al., 2015a). BIX (0.61–0.89) and that FI (1.59–1.82) values were higher during the low flow in both rivers than high flow, suggesting declined production of fresh DOM during the storm events (Table 1). %C1 (46%–64%) in riverine DOM decreased substantially during the high flow in both rivers, whereas %C3 (13%–28%) increased (Table 1). However, no clear trends were observed in the HIX and %C2 values between the two flow periods. The contrasting pattern of increasing $SUVA_{254}$ versus decreasing BIX and FI agreed well with the typical trend in DOM characteristics during storm events in forested (Inamdar et al., 2011; Yang et al., 2015a) and urban watersheds (Lee et al., 2019). Therefore, the riverine DOM during storm events is presumed to be enriched with aromatic and humified DOM constituents, possibly stemming from soil and terrestrial sources. However, a simple comparison of the optical properties between riverine DOM and various end-members is limited in quantifying the relative contributions from the end-members in the catchment. EMMA can facilitate quantitative evaluations.

3.2.4. EMMA using optical descriptors of DOM

A set of DOM optical descriptors including $SUVA_{254}$, HIX, BIX, FI, %C1, %C2, and %C3 were considered for EMMA on the basis of (1) their applicability in the literature and (2) their independent nature or normalization with DOC concentration (Derrien et al., 2018; Derrien et al., 2020; Lee et al., 2019; Yang et al., 2015a). $SUVA_{254}$, BIX, and %C1 values in the rivers were not within the range of end-member values; thus, they were excluded from EMMA (Table 1). HIX and %C2 were also excluded because differences between the low- and high-flow samples were not statistically significant. Finally, FI and %C3 were selected as the most suitable parameters for EMMA because the values of riverine samples were within the end-member range and showed good discrimination between the low- and high-flow samples in the *t*-test ($p < 0.05$) (Table 1; Fig. 3a).

EMMA conducted with FI and %C3 using SIAR revealed major contributions from manure and field soil in the rivers of the agricultural watershed, regardless of the flow season. However, distinct patterns were observed in the contributions of the low- and high-flow riverine DOM (Figs. 3b, S4, S5). The contribution of litter end-members decreased from 19% to 3% in the GH and from 23% to 18% in the HS during the high-flow period (Fig. 3b). The contribution from the reed DOM also decreased from 18% to 2% in the GH and from 24% to 15% in the HS. By contrast, field soil (23%–38%) and manure (30%–56%) exhibited greater contributions to the high-flow riverine DOM than litter and reed because of the higher accessibility of DOM leaching from the manure-applied soil in the watershed (Inamdar et al., 2011; Lee et al., 2019). Although the two rivers belong to the same watershed, contributions of the two end-members varied between the rivers, presumably because of their different land use and hydrology (Fig. 3b; Table S1). For instance, the contribution from the manure end-member increased drastically in the GH during the storm event, whereas the contribution of field soil was greater in the HS than in the GH. Both sub-catchments are occupied by forest lands (>70%), but agricultural lands are much more dominant in the GH (15.5%) than in the HS catchment (3.5%), which can cause a higher contribution of manure to the GH (Fig. 3b). DON concentration in the manure (1.83 mg g^{-1}) was much higher than those in the soil (0.02 mg g^{-1}) and litter (0.54 mg g^{-1}) end-members, consistent with the EMMA results. The highest DON concentration observed in reed WEOM (3.48 mg g^{-1}) was contradictory to a previous study reporting highest C/N ratio in humic fraction of reed and riparian plant WEOM in agricultural watersheds (Lee et al., 2020).

The EMMA results from the IsoSource program with the same set of optical tracers (i.e., FI and %C3) as input parameters showed predominant input from the field soil but failed to provide reasonable estimates of the contribution from the manure end-member (Fig. 3c). The variability in end-member contributions between low and high flow did not conform with the patterns found in the SIAR model and the frequent use of manure as agricultural activities. For example, the contribution from field soil end-members during a storm event usually increases due to enhanced leaching and flushing of soil DOM with surface runoff and subsurface flow (Inamdar et al., 2012; Inamdar et al., 2011; Lee et al., 2019; Yang et al., 2015a); however, the IsoSource model exhibited a decrease in field soil contribution from low to high flow (Fig. 3c). SIAR model outputs (Fig. 3b) including the proportion density plots (Figs. S4, S5) clearly show the distinct contribution of each end-member DOM during low flow versus high flow. Therefore, the SIAR model performs better than the IsoSource model in this study

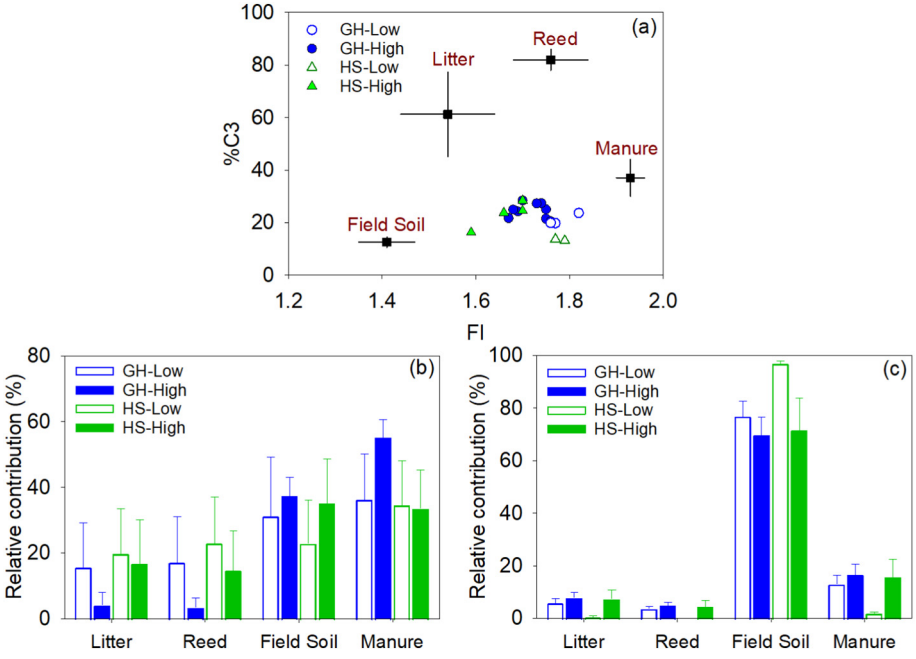

Fig. 3. End-member mixing analysis (EMMA) plot based on FI and %C3 (a). Relative contributions of organic matter sources to storm samples estimated from the EMMA model using Stable Isotope Analysis in R (SIAR) (b) and IsoSource program (c). Go-Hyeon (GH) and Ha-Song (HS) rivers during low and high flow are distinguished by different symbols.

with only four end-members and two small rivers in the Bohyunsan watershed where agricultural practices are active.

3.3. Molecular composition of the end-member and riverine DOM

The detected molecular formulas ranged between 4181 and 7303 in the GH and 3032–7780 in the HS, much lower than the field soil (7883) and manure (11139) end-members (Fig. 4, Table S7). CHO compounds were the most abundant in both rivers, followed by CHON, CHOS, and CHONS (Fig. 5; Table S7). DOM in the GH is abundant with CHO compounds (27%–81%), except for peak discharge (14%), and CHON formulas were more dominant during the peak discharge (47%) (Fig. 5). In the HS, the number of CHON formulas increased during the high-flow period up to 67%, and the CHO formulas decreased (Fig. 5). A relatively smaller but distinct increase in the number of CHONS molecular formulas was also observed in the GH (up to 35% in peak flow) and the HS (11%) during the high-flow period. The abundant CHON formulas in peak discharge provide evidence of additional DON inputs from the manure or manure-applied field soil, which contained many CHON formulas (37% and 45%, respectively) than the litter (21%) and reed (31%) DOM end-members (Fig. 5). The abundance of N-containing formulas (CHON + CHONS) in manure DOM (65%) is consistent with the high DON concentration (Figs. 4 and 5; Tables 1 and S7). Higher fractions of N formulas in riverine DOM under peak discharge indicate substantial export of DON from the field soil and manure to the receiving rivers (Pang et al., 2021; Wagner et al., 2015). A study in agricultural watersheds reported a high abundance of CHON in manure and manure-impacted soil, with high biodegradability of DON (Luek et al., 2020). Another study also confirmed the leaching of DON from the biological transformation of inorganic N fertilizers in a controlled soil experiment (Lusk and Toor, 2016). This finding suggests that active transformation of inorganic N content in manure by plants and microbes could enhance DON export from the catchment to the rivers (Ardón et al., 2010; Lusk and Toor, 2016).

Among the detected molecular formulas, highly unsaturated hydrocarbons were the most abundant biomolecular compounds in the rivers, followed by polyphenols, aliphatic hydrocarbons, and CAS (Fig. S6; Table S7). Variability in DOM molecular composition was observed in the CAS and polyphenol compounds between low- and high-flow samples. In the GH, CAS compounds increased from 5.5% to 7.4% on average from low to high flow, and the increase in polyphenols ranged from 13.5% to 15.5% (Fig. S6; Table S7). In the HS, changes between low flow and high flow were more drastic as CAS compounds increased from 6.4% to 12.0% and polyphenols increased from 14.9% to 18.7% (Fig. S6; Table S7). These increases in CAS and polyphenol compounds in the riverine DOM suggest a predominant contribution from the field soil and manure end-members during peak flow, containing higher CAS (20.8% and 13.2%, respectively) and polyphenols (22.4 and 29.3%), as opposed to litter (<15%) and reed end-members (<10%) (Fig. S6). Although the GH subcatchment has more agricultural land use than that of the HS, the detailed molecular composition can differ, as we observed in this case. Nevertheless, the abundance of CAS compounds in the end-members and the two rivers supports our finding from EMMA that field soil and manure are the predominant contributors of riverine DOM in the agricultural watershed. Although no study has reported enhanced CAS compounds in DOM from agricultural watersheds, a high abundance of polyphenols was reported in the Yangtze basin during the high-flow period (Pang et al., 2021).

3.4. Comparisons between end-members and riverine DOM

The detected molecular formulas were compared between the river samples and end-members, and 536 formulas were commonly present in the DOM of all samples. Among the river samples, 825 and 641 common

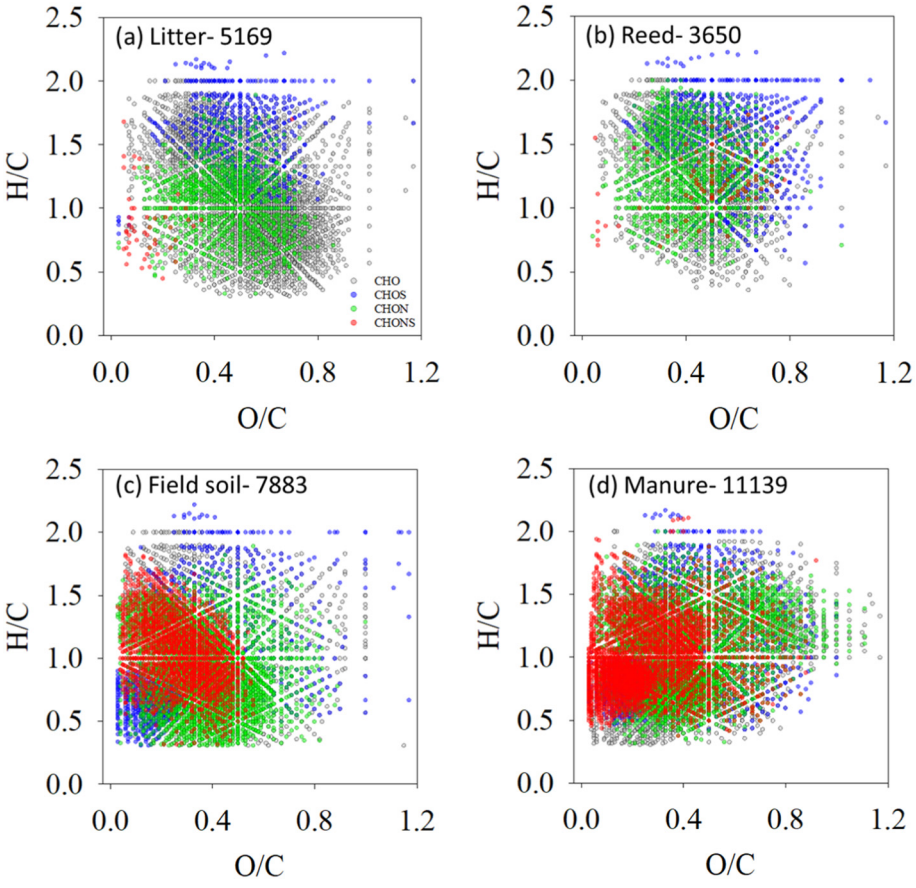

Fig. 4. Van Krevelen diagrams of the detected molecular formulas in litter (a), reed (b), field soil (c), and manure (d) end-members.

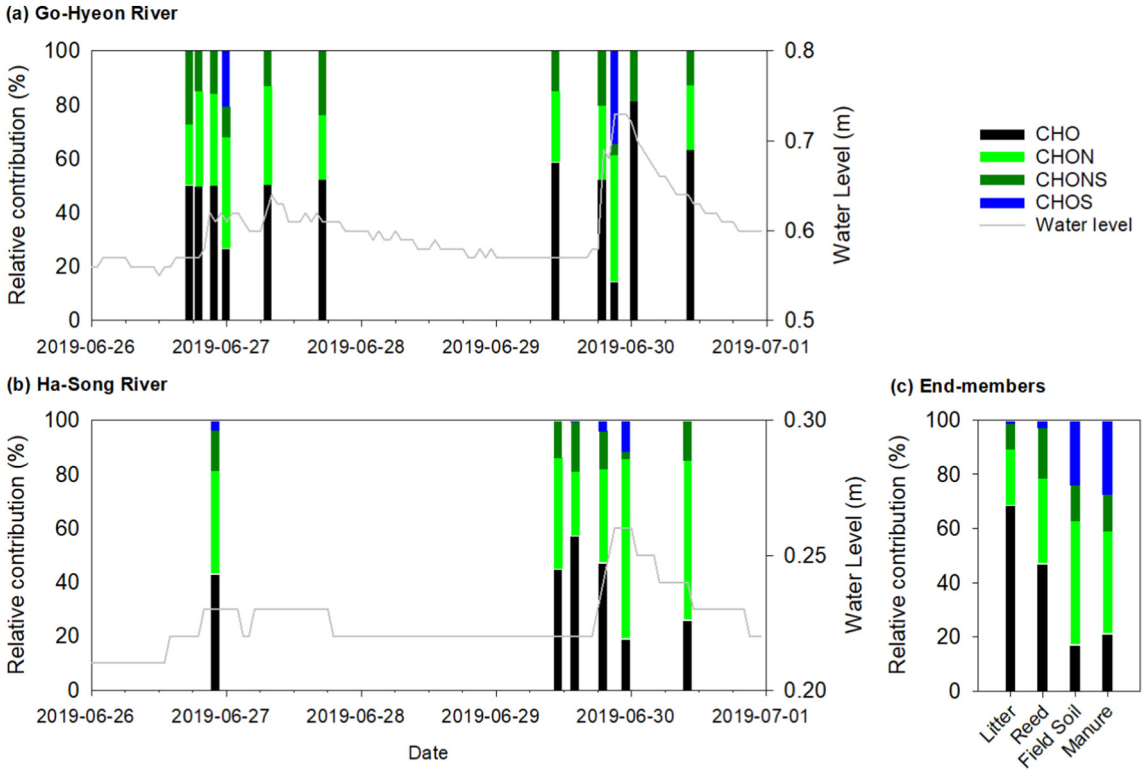

Fig. 5. Relative abundance of molecular groups identified from FT-ICR-MS analysis in the Go-Hyeon (a) and Ha-Song (b) rivers and the four end-members (c).

formulas in the GH and the HS, respectively, were observed. Such common formulas can represent the refractory (termed "stable") fraction of DOM over the period (Figs. 6 and 7). Molecular formulas present in two or more riverine DOM samples were considered semi-labile and were termed as "resistant". Unique or newly identified molecular formulas in each of the riverine DOM samples were termed as "unique" formulas. In the GH, the

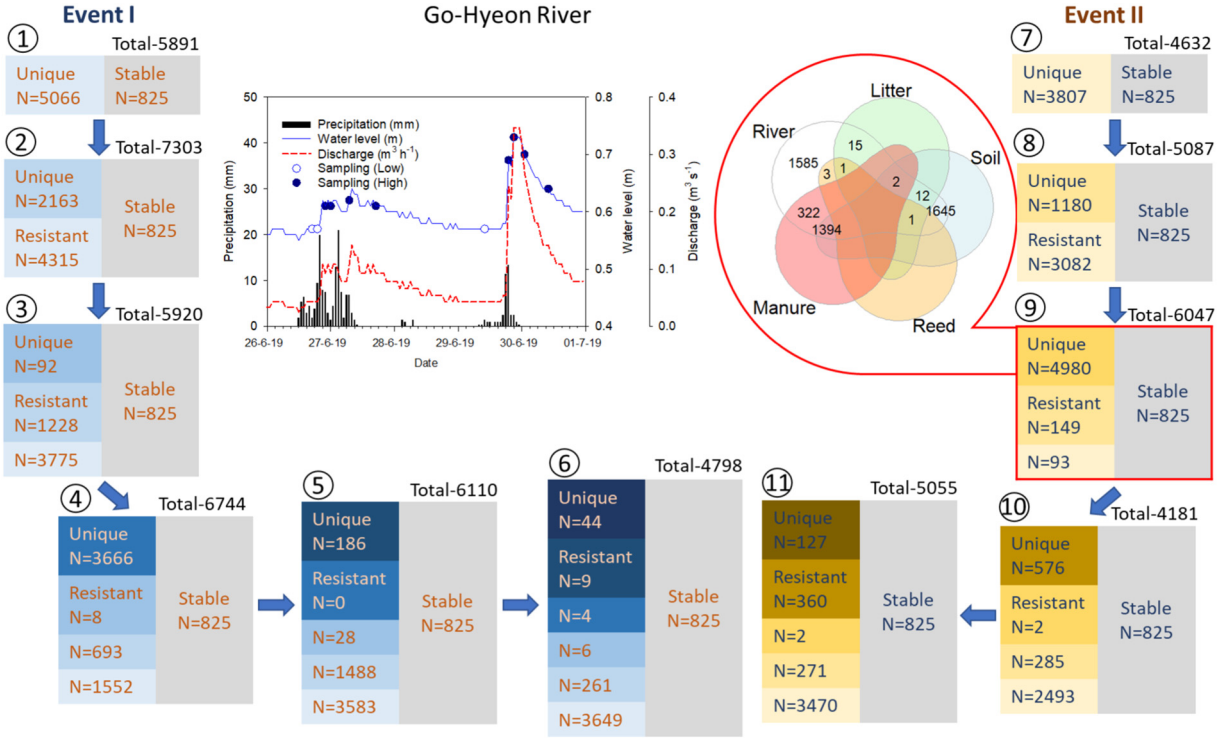

Fig. 6. Stable (common), resistant (common in ≥2 samples), and unique molecular formulas during two consecutive storm events that affected the Go-Hyeon River. Total molecular formulas and sampling times are included above each box. Similarities between the end-members and the unique molecular formulas from the peak flow (#9) are shown in a Venn diagram.

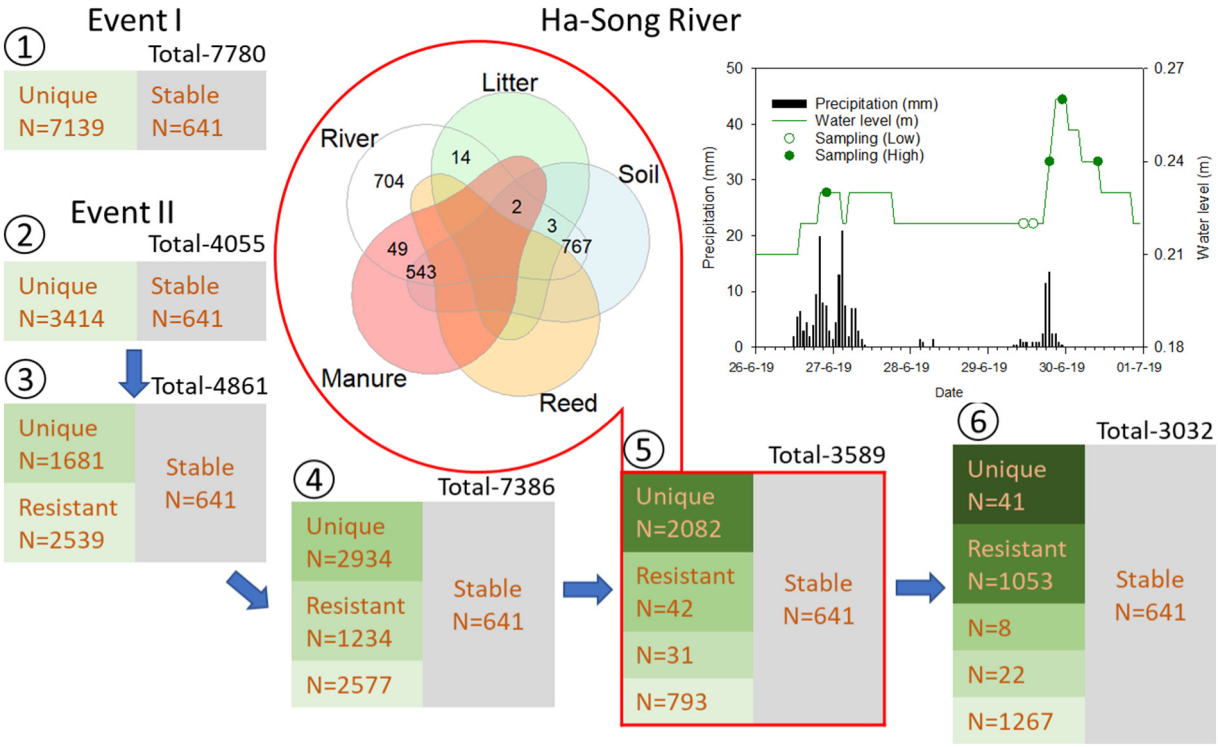

Fig. 7. Stable (common), resistant (common in ≥2 samples), and unique molecular formulas during the storm events in the Ha-Song River. Total molecular formulas and sampling times are included above each box. Similarities between the end-members and the unique molecular formulas from the peak flow (#5) are shown in a Venn diagram.

number of resistant DOM formulas in the low-flow samples (i.e., #1 and #7) and the high-flow samples ranged from 1552 to 3775 and from 2493 to 3470 during the first and the second storm events, respectively, except for the peak discharge (#9) (Fig. 6). The DOM molecular composition in the peak discharge (#9) exhibited an unusually large number of unique molecular formulas (>4980 formulas), indicating newly added allochthonous DOM through surface runoff and subsurface leaching during the peak discharge (Pang et al., 2021). In the HS, the resistant molecular formulas from low-flow (#2) and high-flow samples ranged from 1267 to 2577, and DOM in the peak discharge sample featured 2082 unique formulas (Fig. 7). When the DOM composition of the end-members was compared with the unique molecular formulas in the peak flow, it was evident that contributions from manure (1718 and 594) and field soil (3054 and 1315) end-members were predominant in the GH and the HS (Figs. 4 and 6). However, approximately 30% of the unique molecular formulas in the GH (1585) and the HS (704) during the peak flow were not found in any of the four end-members, which can be explained by either the (1) presence of an additional source of DOM in the catchment (e.g., riparian plants, algae, groundwater, and deep soil), (2) occurrence of fresh DOM produced in situ from microbial exudates, (3) breaking down of complex lignin compounds, or (4) aggregation of smaller molecules (Benner and Biddanda, 1998; Romera-Castillo et al., 2014; Ward et al., 2013). A study implied additional contributions from different soil layers, such as increasing input from deep soil in riverine DOM during peak flow (Lee et al., 2019). Similarly, many unique molecular formulas have been reported in the Yangtze River, mainly ascribed to products from lignin degradation, leached from a soil DOM pool during a high-flow period (Pang et al., 2021). These findings indicate that using only four end-members might be insufficient to track the DOM source, particularly in large river systems with multiple anthropogenic stresses. Therefore, careful evaluation is necessary for selecting end-members for accurate mixing model outputs. Furthermore, the Bayesian mixing model provides the optimum solution to end-member DOM contributions to rivers, unlike the linear mixing models, which provide a range of feasible solutions (Wang et al., 2019). However, the SIAR program can fit a model even if the mixture values (riverine DOM) remain outside the mixing polygon of source signatures (end-member DOM); thus, data should be evaluated carefully before attempting to model in SIAR (Parnell et al., 2010). Despite these limitations, quantification of the contribution of end-members by EMMA models coupled with the molecular composition of DOM in the small agricultural watershed provided a clear indication of the impact of manure on field soil and riverine DON pool.

3.5. Comparison between optical properties-based EMMA and FT-ICR-MS results

The predominant end-member contribution from field soil and manure found in EMMA using DOM optical descriptors were consistent with FT-ICR-MS results (Figs. 3, 6, 7). For example, a relatively higher number of CHON, CHONS, CAS, and polyphenols formulas found in peak flow were similar to those of field soil and manure (Figs. 5, S6). The similarity analysis of DOM molecular composition between riverine DOM also revealed that a large number of the unique molecular formulas were introduced during peak flow (Figs. 6, 7). Over 60% of these unique molecular formulas came directly from the field soil and manure end-members. In addition, a principal component analysis (PCA, performed in R with vegan package) also displayed clear clusters of low and high flow samples (Fig. S7). The two major principal components explained 64% of the total variance. High flow samples were aligned along the PC1 (40.4%) suggesting close association with field soil and manure end-members as well as with CHON, CHONS, CAS, and polyphenols formulas (Fig. S7; Table S8). The two optical descriptors used in EMMA, FI, and %C3 were aligned along the PC3 and PC2, respectively (Fig. S7; Table S8). Litter and reed end-members were scattered indicating relatively smaller contribution to the riverine DOM (Fig. S7), which was consistent with our findings from DOM optical descriptor-based EMMA and similarity analysis of DOM molecular composition. Despite using only four end-members, which is the minimum number of sources required for SIAR model, the enhanced export of DON from manure-impacted agricultural watershed was revealed by combining DOM optical and molecular compositions. However, including more DOM end-members such as algae, sediments, and ground

water will increase the accuracy of the EMMA (Lee et al., 2019; Lee et al., 2020).

3.6. Environmental implications of DON

Management of DIN has been reported in agricultural and urban watersheds to improve water quality by controlling eutrophication, harmful algal blooms, and greenhouse gas emissions (Chun et al., 2020; Smith et al., 1999). However, many studies have reported a significant contribution of DON to agricultural runoff affected by inorganic fertilizer or manure (Graeber et al., 2015; Hussain et al., 2020; Li et al., 2018; Luek et al., 2020; Manninen et al., 2018). High DON concentrations can interfere with instream processes, such as nitrification and ammonification, and change N transformations in affected rivers (Li et al., 2018). DON used to be considered available only for bacteria, but studies have provided evidence of planktonic uptake of DON, particularly in DIN-depleted environments (Berthelot et al., 2021; Bronk et al., 2007). The relatively low concentration range of DON observed in the small Bohyunsan watershed might be much more pronounced in watersheds heavily affected by agricultural activities. Therefore, the rising N pollution in agricultural watersheds worldwide warrants further research on the source, composition, and control of DON at higher spatial and temporal resolutions to complement the knowledge on DIN and for improved management of N leaching.

4. Conclusion

Source tracking of DOM in two rivers of an agricultural watershed revealed enhanced contribution from manure and manure-impacted field soil to the riverine DOM, particularly during peak flow of storm events. The predominant contribution of manure DOM in the rivers quantified by EMMA with optical descriptors was consistent with the molecular composition of DOM. Increases in CHON and CHONS formulas up to 67% and 35%, respectively, and a decrease in the CHO formulas during the peak flow suggest a significant alteration in the end-members contribution to DON. Similarity analysis for molecular composition also confirmed that manure and field soil were the major sources of the molecular formulas uniquely contained in riverine DOM during peak flow. Many studies have focused solely on DIN export from agricultural catchments due to the use of inorganic fertilizers; however, manure application has been considered a frequently used alternative to N and P fertilizers without paying much attention to DON leaching from the watershed. Therefore, this study provides useful insights into the environmental implications of DON in anthropogenically impacted river systems. Due to changing climate with an increase in precipitation in the tropical and temperate regions, the leaching of DON might be enhanced further and cause challenging environmental problems associated with DON.

CRediT authorship contribution statement

Most Shirina Begum: Conceptualization, Methodology, Investigation, Data curation, Investigation, Visualization, Writing - Original draft preparation.

Mi-Hee Lee: Writing - Reviewing and Editing, Investigation, Validation.

Tae Jun Park: Investigation, Data curation.

Seung Yoon Lee: Methodology, Investigation, Reviewing.

Kyung-Hoon Shin: Conceptualization, Reviewing.

Hyun-Sang Shin: Methodology, Reviewing.

Meilian Chen: Writing - Reviewing and Editing.

Jin Hur: Supervision, Resources, Project Administration, Funding acquisition, Conceptualization, Writing - Reviewing and Editing.

Declaration of competing interest

The authors declare that they have no competing financial interests or personal relationships that could have influenced the work reported in this paper.

Acknowledgments

This work was supported by the National Research Foundation of Korea, funded by the Korean Government [grant number 2020R1A4A2002823]. Additional support was provided by the Korea Environment Industry & Technology Institute (KEITI) through the program for the management of aquatic ecosystem health, funded by the Korea Ministry of Environment (MOE) [grant number 2020003030005].

Appendix A. Supplementary data

Supplementary data to this article can be found online at https://doi.org/10.1016/j.scitotenv.2021.152183.

References

Ardón, M., Morse, J.L., Doyle, M.W., Bernhardt, E.S., 2010. The water quality consequences of restoring wetland hydrology to a large agricultural watershed in the Southeastern Coastal Plain. Ecosystems 13 (7), 1060–1078.

Aufdenkampe, A.K., Mayorga, E., Raymond, P.A., Melack, J.M., Doney, S.C., Alin, S.R., Aalto, R.E., Yoo, K., 2011. Riverine coupling of biogeochemical cycles between land, oceans, and atmosphere. Front. Ecol. Environ. 9 (1), 53–60.

Bauer, J.E., Bianchi, T.S., 2011. Treatise on Estuarine and Coastal Science, pp. 7–67.

Begum, M.S., Jang, I., Lee, J.M., Oh, H.B., Jin, H., Park, J.H., 2019. Synergistic effects of urban tributary mixing on dissolved organic matter biodegradation in an impounded river system. Sci. Total Environ. 676, 105–119.

Benner, R., Biddanda, B., 1998. Photochemical transformations of surface and deep marine dissolved organic matter: effects on bacterial growth. Limnol. Oceanogr. 43 (6), 1373–1378.

Berthelot, H., Duhamel, S., L'Helguen, S., Maguer, J.F., Cassar, N., 2021. Inorganic and organic carbon and nitrogen uptake strategies of picoplankton groups in the northwestern Atlantic Ocean. Limnol. Oceanogr. 66 (10), 3682–3696.

Bida, M.R., Tyler, A.C., Pagano, T., 2015. Quantity and composition of stream dissolved organic matter in the watershed of Conesus Lake, New York. J. Great Lakes Res. 41 (3), 730–742.

Bronk, D.A., See, J.H., Bradley, P., Killberg, L., 2007. DON as a source of bioavailable nitrogen for phytoplankton. Biogeosciences 4 (3), 283–296.

Chen, M., He, W., Choi, I., Hur, J., 2016. Tracking the monthly changes of dissolved organic matter composition in a newly constructed reservoir and its tributaries during the initial impounding period. Environ. Sci. Pollut. Res. Int. 23 (2), 1274–1283.

Chen, M., Zeng, C., Zhang, F., Kang, S., Li, C., 2020. Characteristics of dissolved organic matter from a transboundary Himalayan watershed: relationships with land use, elevation, and hydrology. ACS Earth Space Chem. 4 (3), 449–456.

Chen, M., Li, C., Spencer, R.G.M., Maie, N., Hur, J., McKenna, A.M., Yan, F., 2021. Climatic, land cover, and anthropogenic controls on dissolved organic matter quantity and quality from major alpine rivers across the Himalayan-Tibetan Plateau. Sci. Total Environ. 754, 142411.

Chun, Y., Kim, D., Hattori, S., Toyoda, S., Yoshida, N., Huh, J., Lim, J.H., Park, J.H., 2020. Temperature control on wastewater and downstream nitrous oxide emissions in an urbanized river system. Water Res. 187, 116417.

Cole, J.J., Prairie, Y.T., Caraco, N.F., McDowell, W.H., Tranvik, L.J., Striegl, R.G., Duarte, C.M., Kortelainen, P., Downing, J.A., Middelburg, J.J., Melack, J., 2007. Plumbing the global carbon cycle: integrating inland waters into the terrestrial carbon budget. Ecosystems 10 (1), 172–185.

Cory, R.M., Miller, M.P., McKnight, D.M., Guerard, J.J., Miller, P.L., 2010. Effect of instrument-specific response on the analysis of fulvic acid fluorescence spectra. Limnol. Oceanogr. Methods 8 (2), 67–78.

Derrien, M., Kim, M.S., Ock, G., Hong, S., Cho, J., Shin, K.H., Hur, J., 2018. Estimation of different source contributions to sediment organic matter in an agricultural-forested watershed using end member mixing analyses based on stable isotope ratios and fluorescence spectroscopy. Sci. Total Environ. 618, 569–578.

Derrien, M., Brogi, S.R., Goncalves-Araujo, R., 2019. Characterization of aquatic organic matter: assessment, perspectives and research priorities. Water Res. 163, 114908.

Derrien, M., Lee, M.H., Choi, K., Lee, K.S., Hur, J., 2020. Tracking the evolution of particulate organic matter sources during summer storm events via end-member mixing analysis based on spectroscopic proxies. Chemosphere 252, 126445.

Fellman, J.B., Hood, E., Spencer, R.G.M., 2010. Fluorescence spectroscopy opens new windows into dissolved organic matter dynamics in freshwater ecosystems: a review. Limnol. Oceanogr. 55 (6), 2452–2462.

Graeber, D., Boechat, I.G., Encina-Montoya, F., Esse, C., Gelbrecht, J., Goyenola, G., Gucker, B., Heinz, M., Kronvang, B., Meerhoff, M., Nimptsch, J., Pusch, M.T., Silva, R.C., von Schiller, D., Zwirnmann, E., 2015. Global effects of agriculture on fluvial dissolved organic matter. Sci. Rep. 5, 16328.

Harrison, J.A., Caraco, N., Seitzinger, S.P., 2005. Global patterns and sources of dissolved organic matter export to the coastal zone: results from a spatially explicit, global model. Glob. Biogeochem. Cycles 19 (4) n/a-n/a.

He, W., Choi, I., Lee, J.J., Hur, J., 2016. Coupling effects of abiotic and biotic factors on molecular composition of dissolved organic matter in a freshwater wetland. Sci. Total Environ. 544, 525–534.

Hounshell, A.G., Peierls, B.L., Osburn, C.L., Paerl, H.W., 2017. Stimulation of phytoplankton production by anthropogenic dissolved organic nitrogen in a coastal plain estuary. Environ. Sci. Technol. 51 (22), 13104–13112.

Huguet, A., Vacher, L., Relexans, S., Saubusse, S., Froidefond, J.M., Parlanti, E., 2009. Properties of fluorescent dissolved organic matter in the Gironde Estuary. Org. Geochem. 40 (6), 706–719.
Hussain, M.Z., Robertson, G.P., Basso, B., Hamilton, S.K., 2020. Leaching losses of dissolved organic carbon and nitrogen from agricultural soils in the upper US Midwest. Sci. Total Environ. 734, 139379.
Inamdar, S., Singh, S., Dutta, S., Levia, D., Mitchell, M., Scott, D., Bais, H., McHale, P., 2011. Fluorescence characteristics and sources of dissolved organic matter for stream water during storm events in a forested mid-Atlantic watershed. J. Geophys. Res. 116 (G3).
Inamdar, S., Finger, N., Singh, S., Mitchell, M., Levia, D., Bais, H., Scott, D., McHale, P., 2012. Dissolved organic matter (DOM) concentration and quality in a forested mid-Atlantic watershed, USA. Biogeochemistry 108 (1–3), 55–76.
Ittekkot, V., Safiullah, S., Mycke, B., Seifert, R., 1985. Seasonal variability and geochemical significance of organic-matter in the River Ganges,Bangladesh. Nature 317 (6040), 800–802.
Jiang, R., Hatano, R., Zhao, Y., Kuramochi, K., Hayakawa, A., Woli, K.P., Shimizu, M., 2014. Factors controlling nitrogen and dissolved organic carbon exports across timescales in two watersheds with different land uses. Hydrol. Process. 28 (19), 5105–5121.
Jung, B.J., Lee, J.K., Kim, H., Park, J.H., 2014. Export, biodegradation, and disinfection byproduct formation of dissolved and particulate organic carbon in a forested headwater stream during extreme rainfall events. Biogeosciences 11 (21), 6119–6129.
Knapik, H.G., Fernandes, C.V., de Azevedo, J.C., dos Santos, M.M., Dall'Agnol, P., Fontane, D.G., 2015. Biodegradability of anthropogenic organic matter in polluted rivers using fluorescence, UV, and BDOC measurements. Environ. Monit. Assess. 187 (3), 104.
Koch, B.P., Dittmar, T., 2006. From mass to structure: an aromaticity index for high-resolution mass data of natural organic matter. Rapid Commun. Mass Spectrom. 20 (5), 926–932.
Koch, B.P., Dittmar, T., 2016. From mass to structure: an aromaticity index for high-resolution mass data of natural organic matter. Rapid Commun. Mass Spectrom. 30 (1), 250.
Lawaetz, A.J., Stedmon, C.A., 2009. Fluorescence intensity calibration using the raman scatter peak of water. Appl. Spectrosc. 63 (8), 936–940.
Lee, M.-H., Payeur-Poirier, J.-L., Park, J.-H., Matzner, E., 2016. Variability in runoff fluxes of dissolved and particulate carbon and nitrogen from two watersheds of different tree species during intense storm events. Biogeosciences 13 (18), 5421–5432.
Lee, M.H., Lee, Y.K., Derrien, M., Choi, K., Shin, K.H., Jang, K.S., Hur, J., 2019. Evaluating the contributions of different organic matter sources to urban river water during a storm event via optical indices and molecular composition. Water Res. 165, 115006.
Lee, M.-H., Lee, S.Y., Yoo, H.-Y., Shin, K.-H., Hur, J., 2020. Comparing optical versus chromatographic descriptors of dissolved organic matter (DOM) for tracking the non-point sources in rural watersheds. Ecol. Indic. 117.
Lewis, W.M., Wurtsbaugh, W.A., Paerl, H.W., 2011. Rationale for control of anthropogenic nitrogen and phosphorus to reduce eutrophication of inland waters. Environ. Sci. Technol. 45 (24), 10300–10305.
Li, L., He, Z., Li, Z., Zhang, S., Li, S., Wan, Y., Stoffella, P.J., 2016. Spatial and temporal variation of nitrogen concentration and speciation in runoff and storm water in the Indian River watershed, South Florida. Environ. Sci. Pollut. Res. Int. 23 (19), 19561–19569.
Li, L., He, Z.L., Tfaily, M.M., Inglett, P., Stoffella, P.J., 2018. Spatial-temporal variations of dissolved organic nitrogen molecular composition in agricultural runoff water. Water Res. 137, 375–383.
Luek, J.L., Brooker, M.R., Ash, B.L., Robert Midden, W., Mouser, P.J., 2020. Seasonal changes predominant over manure application in driving dissolved organic matter shifts in agricultural runoff. J. Great Lakes Res. 46 (6), 1570–1580.
Lusk, M.G., Toor, G.S., 2016. Dissolved organic nitrogen in urban streams: biodegradability and molecular composition studies. Water Res. 96, 225–235.
Manninen, N., Soinne, H., Lemola, R., Hoikkala, L., Turtola, E., 2018. Effects of agricultural land use on dissolved organic carbon and nitrogen in surface runoff and subsurface drainage. Sci. Total Environ. 618, 1519–1528.
McCallister, S.L., Ishikawa, N.F., Kothawala, D.N., 2018. Biogeochemical tools for characterizing organic carbon in inland aquatic ecosystems. Limnol. Oceanogr. Lett. 3 (6), 444–457.
McKnight, D.M., Boyer, E.W., Westerhoff, P.K., Doran, P.T., Kulbe, T., Andersen, D.T., 2001. Spectrofluorometric characterization of dissolved organic matter for indication of precursor organic material and aromaticity. Limnol. Oceanogr. 46 (1), 38–48.
Menges, J., Hovius, N., Andermann, C., Lupker, M., Haghipour, N., Märki, L., Sachse, D., 2020. Variations in organic carbon sourcing along a trans-Himalayan river determined by a Bayesian mixing approach. Geochim. Cosmochim. Acta 286, 159–176.
Murphy, K.R., Stedmon, C.A., Wenig, P., Bro, R., 2014. OpenFluor– an online spectral library of auto-fluorescence by organic compounds in the environment. Anal. Methods 6 (3), 658–661.
Ohno, T., 2002. Fluorescence inner-filtering correction for determining the humification index of dissolved organic matter. Environ. Sci. Technol. 36 (4), 742–746.
Osburn, C.L., Handsel, L.T., Peierls, B.L., Paerl, H.W., 2016. Predicting sources of dissolved organic nitrogen to an estuary from an agro-urban coastal watershed. Environ. Sci. Technol. 50 (16), 8473–8484.
Pagano, T., Bida, M., Kenny, J., 2014. Trends in levels of allochthonous dissolved organic carbon in natural water: a review of potential mechanisms under a changing climate. Water 6 (10), 2862–2897.
Pang, Y., Wang, K., Sun, Y., Zhou, Y., Yang, S., Li, Y., He, C., Shi, Q., He, D., 2021. Linking the unique molecular complexity of dissolved organic matter to flood period in the Yangtze River mainstream. Sci. Total Environ. 764, 142803.
Park, J.-H., Nayna, O.K., Begum, M.S., Chea, E., Hartmann, J., Keil, R.G., Kumar, S., Lu, X., Ran, L., Richey, J.E., Sarma, V.V.S.S., Tareq, S.M., Xuan, D.T., Yu, R., 2018. Reviews and syntheses: anthropogenic perturbations to carbon fluxes in asian river systems – concepts, emerging trends, and research challenges. Biogeosciences 15 (9), 3049–3069.
Parnell, A.C., Inger, R., Bearhop, S., Jackson, A.L., 2010. Source partitioning using stable isotopes: coping with too much variation. PLoS One 5 (3), e9672.
Pellerin, B.A., Kaushal, S.S., McDowell, W.H., 2006. Does anthropogenic nitrogen enrichment increase organic nitrogen concentrations in runoff from forested and human-dominated watersheds? Ecosystems 9 (5), 852–864.
Pisani, O., Boyer, J.N., Podgorski, D.C., Thomas, C.R., Coley, T., Jaffé, R., 2017. Molecular composition and bioavailability of dissolved organic nitrogen in a lake flow-influenced river in south Florida, USA. Aquat. Sci. 79 (4), 891–908.
Raymond, P.A., Saiers, J.E., Sobczak, W.V., 2016. Hydrological and biogeochemical controls on watershed dissolved organic matter transport: pulse-shunt concept. Ecology 97 (1), 5–16.
Romera-Castillo, C., Chen, M., Yamashita, Y., Jaffe, R., 2014. Fluorescence characteristics of size-fractionated dissolved organic matter: implications for a molecular assembly based structure? Water Res. 55, 40–51.
See, J.H., Bronk, D.A., Lewitus, A.J., 2006. Uptake of spartina-derived humic nitrogen by estuarine phytoplankton in nonaxenic and axenic culture. Limnol. Oceanogr. 51 (5), 2290–2299.
Seitzinger, S.P., Sanders, R.W., Styles, R., 2002. Bioavailability of DON from natural and anthropogenic sources to estuarine plankton. Limnol. Oceanogr. 47 (2), 353–366.
Sipler, R.E., Bronk, D.A., 2015. Biogeochemistry of Marine Dissolved Organic Matter, pp. 127–232.
Smith, V.H., Tilman, G.D., Nekola, J.C., 1999. Eutrophication: impacts of excess nutrient inputs on freshwater, marine, and terrestrial ecosystems. Environ. Pollut. 100 (1–3), 179–196.
Spencer, R.G.M., Guo, W., Raymond, P.A., Dittmar, T., Hood, E., Fellman, J., Stubbins, A., 2014. Source and biolability of ancient dissolved organic matter in glacier and lake ecosystems on the Tibetan Plateau. Geochim. Cosmochim. Acta 142, 64–74.
Spencer, R.G.M., Kellerman, A.M., Podgorski, D.C., Macedo, M.N., Jankowski, K., Nunes, D., Neill, C., 2019. Identifying the molecular signatures of agricultural expansion in Amazonian headwater streams. J. Geophys. Res. Biogeosci. 124 (6), 1637–1650.
Stedmon, C.A., Bro, R., 2008. Characterizing dissolved organic matter fluorescence with parallel factor analysis: a tutorial. Limnol. Oceanogr.Methods 6, 572–579.
Tewfik, A., Bell, S.S., McCann, K.S., Morrow, K., 2016. Predator diet and trophic position modified with altered habitat morphology. PLoS One 11 (1), e0147759.
Wagner, S., Riedel, T., Niggemann, J., Vahatalo, A.V., Dittmar, T., Jaffe, R., 2015. Linking the molecular signature of heteroatomic dissolved organic matter to watershed characteristics in world rivers. Environ. Sci. Technol. 49 (23), 13798–13806.
Wang, J., Lu, N., Fu, B., 2019. Inter-comparison of stable isotope mixing models for determining plant water source partitioning. Sci. Total Environ. 666, 685–693.
Ward, N.D., Keil, R.G., Medeiros, P.M., Brito, D.C., Cunha, A.C., Dittmar, T., Yager, P.L., Krusche, A.V., Richey, J.E., 2013. Degradation of terrestrially derived macromolecules in the Amazon River. Nat. Geosci. 6 (7), 530–533.
Wehrli, B., 2013. BIOGEOCHEMISTRY conduits of the carbon cycle. Nature 503 (7476), 346–347.
Weishaar, J.L., Aiken, G.R., Bergamaschi, B.A., Fram, M.S., Fujii, R., Mopper, K., 2003. Evaluation of specific ultraviolet absorbance as an indicator of the chemical composition and reactivity of dissolved organic carbon. Environ. Sci. Technol. 37 (20), 4702–4708.
Wilson, H.F., Xenopoulos, M.A., 2009. Effects of agricultural land use on the composition of fluvial dissolved organic matter. Nat. Geosci. 2 (1), 37–41.
Xue, D., De Baets, B., Van Cleemput, O., Hennessy, C., Berglund, M., Boeckx, P., 2012. Use of a Bayesian isotope mixing model to estimate proportional contributions of multiple nitrate sources in surface water. Environ. Pollut. 161, 43–49.
Yang, L., Chang, S.-W., Shin, H.-S., Hur, J., 2015a. Tracking the evolution of stream DOM source during storm events using end member mixing analysis based on DOM quality. J. Hydrol. 523, 333–341.
Yang, L., Hur, J., Lee, S., Chang, S.W., Shin, H.S., 2015b. Dynamics of dissolved organic matter during four storm events in two forest streams: source, export, and implications for harmful disinfection byproduct formation. Environ. Sci. Pollut. Res. Int. 22 (12), 9173–9183.
Ye, Q., Zhang, Z.-T., Liu, Y.-C., Wang, Y.-H., Zhang, S., He, C., Shi, Q., Zeng, H.-X., Wang, J.-J., 2019. Spectroscopic and molecular-level characteristics of dissolved organic matter in a highly polluted urban river in South China. ACS EarthSpace Chem. 3 (9), 2033–2044.
Yu, Z., Liu, X., Chen, C., Liao, H., Chen, Z., Zhou, S., 2019. Molecular insights into the transformation of dissolved organic matter during hyperthermophilic composting using ESI FT-ICR MS. Bioresour. Technol. 292, 122007.
Zhang, F., Li, Y., Xiong, X., Yang, M., Li, W., 2012. Effect of composting on dissolved organic matter in animal manure and its binding with Cu. ScientificWorldJournal 2012, 289896.
Zhang, Q., Wang, H., Lu, C., 2020. Tracing sulfate origin and transformation in an area with multiple sources of pollution in northern China by using environmental isotopes and Bayesian isotope mixing model. Environ. Pollut. 265 (Pt B), 115105.
Zhang, L., You, Y., Gao, C., Peng, Y., Cao, Z., 2021. Dissolved organic nitrogen structural and component changes in overlying water along urban river at molecular and material levels — Beiyun basin case study. J. Clean. Prod. 287.
Zsolnay, A., Baigar, E., Jimenez, M., Steinweg, B., Saccomandi, F., 1999. Differentiating with fluorescence spectroscopy the sources of dissolved organic matter in soils subjected to drying. Chemosphere 38 (1), 45–50.